Diagnostic and Interventional Imaging (2019) **100**, 619—634

REVIEW /*Genitourinary imaging*

How to differentiate uterine leiomyosarcoma from leiomyoma with imaging

S. Sun[a,*], **P.A. Bonaffini**[a], **S. Nougaret**[b], **L. Fournier**[c,d], **A. Dohan**[c,e], **J. Chong**[a], **J. Smith**[f], **H. Addley**[f], **C. Reinhold**[a]

[a] *Department of Radiology, McGill University Health Centre, 1001 Decarie boulevard, H4A 3J1 Montreal, QC, Canada*
[b] *Inserm, U1194, Department of Radiology, Montpellier Cancer Institute, University of Montpellier, 34295 Montpellier, France*
[c] *Université de Paris, Descartes-Paris 5, 75006 Paris, France*
[d] *Department of Radiology, Hôpital Européen Georges Pompidou, Assistance Publique—Hôpitaux de Paris, 75015 Paris, France*
[e] *Department of Radiology A, Hôpital Cochin, Assistance Publique—Hôpitaux de Paris, 75014 Paris, France*
[f] *Department of Radiology, Cambridge University Hospitals, NHS Foundation Trust, CB2 0QQ Cambridge, United Kingdom*

KEYWORDS
Leiomyosarcoma;
Leiomyoma;
Differentiation;
Magnetic resonance imaging (MRI);
Uterine tumor

Abstract Uterine leiomyomas, the most frequent benign myomatous tumors of the uterus, often cannot be distinguished from malignant uterine leiomyosarcomas using clinical criteria. Furthermore, imaging differentiation between both entities is frequently challenging due to their potential overlapping features. Because a suspected leiomyoma is often managed conservatively or with minimally invasive treatments, the misdiagnosis of leiomyosarcoma for a benign leiomyoma could potentially result in significant treatment delays, therefore increasing morbidity and mortality. In this review, we provide an overview of the differences between leiomyoma and leiomyosarcoma, mainly focusing on imaging characteristics, but also briefly touching upon their demographic, histopathological and clinical differences. The main indications and limitations of available cross-sectional imaging techniques are discussed, including ultrasound, computed tomography, magnetic resonance imaging (MRI) and positron emission tomography/computed tomography. A particular emphasis is placed on the review of specific

* Corresponding author.
E-mail address: simon.sun@mail.mcgill.ca (S. Sun).

https://doi.org/10.1016/j.diii.2019.07.007

MRI features that may allow distinction between leiomyomas and leiomyosarcomas according to the most recent evidence in the literature. The potential contribution of texture analysis is also discussed. In order to help guide-imaging diagnosis, we provide an MRI-based diagnostic algorithm which takes into account morphological and functional features, both individually and in combination, in an attempt to optimize radiologic differentiation of leiomyomas from leiomyosarcomas.

Uterine leiomyomas, sometimes incorrectly colloquially referred to as uterine fibroids, are the most frequently encountered benign myomatous tumors of the uterus, being observed in up to 20—40% of reproductive-age women and 70—80% of perimenopausal women [1—6]. In addition, these benign tumors may become symptomatic in 20—50% of patients and subsequently produce pelvic pain, subfertility or abnormal uterine bleeding, requiring gynecologic hospitalization in about 30% of affected women [2].

On the malignant spectrum, uterine sarcomas tend to occur in an older patient population when compared to leiomyomas, and only account for 3—7% of all uterine malignancies [7]. They often present with the same symptoms as leiomyomas and thus cannot reliably be distinguished clinically [8—10]. Leiomyosarcomas (LMSs) are the most common uterine sarcomas, with an estimated annual incidence of 0.5—7/100,000 per women, followed by endometrial stromal sarcomas with an annual incidence of 1—2/million per women [7,11—14].

Given that leiomyomas may currently be managed with minimally invasive treatment, it is particularly important to distinguish them preoperatively from confounding malignant entities such as LMSs. This is aimed to avoid inadvertent dissemination by laparoscopic morcellation or delaying diagnosis with conservative management such as uterine artery embolization [3,15—17]. The misdiagnosis of a LMS for a benign leiomyoma could result in treatment delays and greater morbidity, given its poor prognosis and high propensity to locally recur and metastasize [3,18—20].

On the basis of the FIGO 2009 classification, up to 68% of LMSs are diagnosed as stage I and only up to 22% are diagnosed as stage IV (Table 1) [21—24]. Therefore, the imaging characteristics of the primary lesion, rather than secondary signs of malignancy, will ultimately help in differential diagnosis and drive treatment stratification. While relatively rare, uterine LMSs carry a poor prognosis even when confined to the uterus, as they are responsible for a quarter of the deaths from uterine malignancies, with 5-year survival rates ranging from 46—53% [13,25]. Additionally, LMSs also have a 50—70% rate of recurrence, with up to 40% occurring in the lungs and up to 13% in the pelvis [10,19,20,26].

Considering this challenging clinical context and recent advances in magnetic resonance imaging (MRI), multiple attempts have been made to define imaging characteristics for the preoperative differentiation of uterine leiomyomas from LMSs. Although certain imaging features such as ill-defined margins, increased signal intensity on T1- and T2-weighted images, hemorrhage, central necrosis, specific diffusion-weighted imaging (DWI) characteristics and texture analysis histogram metrics have shown promising results, the literature still alludes to equivocal levels of consistency and agreement [3,4,21,22,27—34].

Through this review, we aim to identify and summarize the main imaging features and their efficacy in differentiating uterine leiomyomas from LMSs. A particular emphasis will be placed on the different MRI characteristics of both entities along with their outputs derived from DWI and texture analysis, recent state of the art advances [4,22].

Table 1 FIGO staging for uterine LMS (2009).

Stage	Definition
I	Tumor limited to uterus
IA	<5 cm
IB	>5 cm
II	Tumor extends to the pelvis
IIA	Adnexal involvement
IIB	Tumor extends to involve other pelvic tissues
III	Tumor invades abdominal tissues (more than just protruding into the abdomen)
IIIA	One site
IIIB	More than one site
IIIC	Metastasis to the pelvis and/or para-aortic lymph nodes
IV	
IVA	Invasion of the bladder and/or rectum
IVB	Distant metastasis

Adapted from Prat et al. [91].

Pathology

While differentiating uterine leiomyomas from LMSs on imaging may be challenging, the two neoplasms have separate origins and distinct chromosomal rearrangements, very few of which share enough transcriptional overlap to hypothesize a definite common origin [2,35].

Uterine leiomyomas are benign monoclonal tumors enriched in extracellular matrix, with large amounts of collagen types I—III and disorganized fibril arrangements. They arise from the smooth muscle cells of the myometrium [2,35]. The precise etiology of these tumors remains unclear, but studies have established that factors such as congenitally elevated estrogen receptors in the myometrium, hormonal changes, response to ischemic injury during menses and intrinsic myometrial abnormalities may play a role in initiating causative genetic mutations [2].

Uterine LMSs are a member of the uterine sarcoma category, rare malignant tumors of mesenchymal origin [10,20]. LMSs typically arise de novo given their considerable chromosomal differences in comparison to leiomyomas, although malignant transformation of leiomyoma to LMS has been reported [2,35]. Uterine LMSs are diagnosed on histology based on hypercellularity, severe nuclear atypia and high mitotic rate (greater than 15 mitotic figures per 10 high power fields); however, this is not always clear-cut and a differential diagnosis may need to be entertained [10,36—38]. Potential diagnostic challenges arise due to the existence of epithelioid and myxoid LMS. These are rare, but often aggressive variants with mild atypia, low mitotic rate and frequent absence of necrosis [39,40]. In addition, smooth muscle uterine neoplasms can present only select suspicious histologic features without meeting the full histologic diagnostic criteria of a LMS. In these equivocal cases, they are classified as smooth muscle tumors of uncertain malignant potential (STUMP), which are generally thought to have a favorable prognosis [41].

Hyperactivation of the PI3K/AKT/mTOR pathway, which controls cell proliferation and survival through regulation of gene transcription and protein synthesis has been thought to play a role in the pathogenesis of LMS, with many of them demonstrating phosphorylation of AKT and mTOR [42,43]. Currently there are very scarce clinical reports on targeted treatments for uterine LMS patients although there have been accounts of promising preclinical responses by acting on the PI3K/AKT/mTOR pathway through the combination of mTOR pathway inhibitors with aurora kinase A inhibitors, MDM2 inhibitors or histone deacetylase inhibitors [43].

While there are currently no reliable clinical markers for LMS diagnosis, recent genetic advances have also confirmed frequent alterations in TP53, RB1, α-thalassemia/mental retardation syndrome X-linked (ATRX), and mediator complex subunit 12 (MED12). MED12 in particular, may be helpful for the diagnosis of LMS derived from leiomyoma, which while very rare, tend to have a favorable prognosis [44]. A few overexpressed genes at the primary lesion site (osteocrin, neuroligin 4X, SLITRK4, TSPAN7) are also being investigated [44].

Clinical symptoms

Leiomyomas and LMSs have a very similar clinical presentation, although the mean age at presentation for LMSs (45 years and greater) is usually higher than for leiomyomas (under 45 years). Women with these conditions can present with clinical symptoms such as profuse menstrual bleeding, pelvic discomfort, infertility, increased urinary frequency or incontinence, constipation and dyspareunia [45—47]. Therefore, early distinction of LMS from a benign uterine leiomyoma can prove challenging clinically [24]. While not specific for uterine leiomyomas, cancer antigen 125 (CA125) is elevated in the presence of large (>5 cm) or degenerated subserosal leiomyomas [48,49]. On the other hand, there is no general consensus on the utility of CA125 in the diagnosis of LMS. Juang et al. have found significantly higher preoperative serum CA125 values in patients with LMS than in those with leiomyomas; whereas Menczer at al. found in a series of 17 patients that CA125 was not immunohistochemically expressed in any of their LMS pathologic specimens [50,51]. This raises the possibility that CA125 may sometimes increase due to nonspecific irritation of epithelial surfaces caused by tumor cells [51].

Imaging features

Non-invasive diagnostic imaging has been extensively evaluated to differentiate uterine LMSs from leiomyomas given the important differences in their prognosis and management. Along with standard morphologic imaging tools, including transabdominal ultrasound (TAUS) or transvaginal ultrasound (TVUS), MRI and computed tomography (CT), functional and quantitative techniques, such as diffusion, positron emission tomography/CT (PET/CT) and texture analysis (TA) can also play a role in the initial diagnosis, staging and post treatment evaluation. Moreover, quantitative imaging analysis is now being increasingly used for preoperative prognostic stratification.

Ultrasound

Ultrasound is usually the first imaging modality employed for the detection of uterine myometrial pathology. TVUS is generally preferred as it allows for better evaluation of patients with a retroverted uterus, inadequate bladder distension, significant bowel gas or obese patients. TAUS, however, is superior for assessment of large and fundal leiomyomas [52]. Transvaginal grayscale and color Doppler ultrasound remain easily accessible, radiation free and cost effective for assessment and follow-up of benign uterine leiomyomas. On ultrasound, leiomyomas typically appear as well-defined hypoechoic masses, with possible calcifications resulting in acoustic shadowing. However, it has a limited role in the accurate diagnosis of LMS [2,21,31,52]. Ultrasound is inherently limited by a low depth of penetration and inter-operator variability. Moreover, uterine LMSs and leiomyomas can both demonstrate similar heterogeneous echogenicity and central necrosis, especially in cases of atypical benign lesions [2,52,53]. Although not always reliable, increased vascularity on color Doppler ultrasound can sometimes favor malignancy, especially when combined with a large size and degenerative cystic changes. This combination of findings increases the sensitivity to 75% and positive predictive value to 60% [52,54,55]. Additionally, leiomyomas have a statistically significant lower mean arteriolar resistance index (0.59 ± 0.01 [SD]) in comparison to mixed mesodermal tumors (0.41 ± 0.06 [SD]), although no significant difference was found when comparing the same variable between leiomyomas and LMSs [53].

Table 2 Standard pelvic MRI protocol for leiomyoma/leiomyosarcoma imaging.

T1-weighted sequence in the axial plane
T1-weighted fat-saturated sequence in the axial plane
T2-weighted sequence in the axial plane
T2-weighted sequence in the sagittal plane
T2-weighted sequence in the axial oblique plane
DWI (b1000) with corresponding ADC map
Dynamic contrast-enhanced sequence in plane best depicting the morphology of the lesion

CT

CT plays a limited role in the initial diagnosis and local staging of myometrial lesions. CT is excellent for demonstrating calcifications; they are often found in leiomyomas but may also be present in LMSs [56]. CT can also be useful in the initial evaluation of patients presenting with acute abdominal pain, especially those with torsed subserosal leiomyomas, which can then undergo hemorrhagic necrosis and confound the diagnosis [57,58]. In women with LMS, CT is primarily used for staging purposes and to exclude distant recurrence post therapy (LMS tends to metastasize to the lungs and liver) [59]. CT is also optimal for visualizing the postoperative pelvic anatomy, allowing for proper evaluation of surgical complications including bowel obstruction or injury, ureteral or bladder injuries and urinary fistulas [60].

MRI

Despite equivocal levels of agreement over the diagnostic accuracy of individual features, MRI remains the preferred imaging modality for in-depth evaluation of myomatous uterine tumors and for delineation of local spread of malignant disease [31,61,62].

Patient preparation and MRI protocol

According to the European Society of Urogenital Radiology (ESUR) guidelines, MRI of the pelvis should be performed following a period of fasting (3 to 6 hours) and with a moderately distended urinary bladder to achieve optimal visualization of the pelvis. The administration of an antiperistaltic agent is also recommended in order to optimize image quality. While specific scheduling according to patient's menstrual cycle is not indicated, clinical information relating to the specifics of the patient's menstrual cycle and hormonal status should however be documented. As per the ESUR guidelines, the current standard MRI protocol for the pelvis includes: axial T1-weighted imaging, with fat saturation sequence in the presence of high signal/fat containing lesions; sagittal and axial T2-weighted imaging, with at least two orthogonal oblique planes of the uterus. Diffusion-weighted imaging (DWI) and dynamic contrast-enhanced (DCE) imaging should always be included when assessing an indeterminate myometrial mass (Table 2) [63]. Signal intensity characteristics of myometrial lesions on T1-weighted sequences are defined in comparison to the fatty bone marrow in the pubic symphysis, while on T2-weighted sequences they are defined in comparison to the outer myometrium. Finally, signal intensity on DWI is defined in comparison to the endometrium: high signal represents equal or higher signal than the endometrium [34,64].

Classic morphologic MRI features

On MRI, typical uterine leiomyomas present as well-delineated masses of variable size that may be solitary or multifocal, with low signal intensities on T1- and T2-weighted images; this is mainly due to their increased proportion of smooth muscle content [34,63,65,66]. They range in size from 10 mm to 20 cm, taking into account that most available imaging techniques cannot accurately help characterize lesions smaller than 10 mm [2,5,35]. Currently, leiomyomas are classified according to the International Federation of Obstetrics and Gynecology (FIGO) classification, mainly based on their location relative to the uterus [5,67]. Leiomyomas generally tend to demonstrate low apparent diffusion coefficient (ADC) values, but in the presence of cystic or myxomatous degeneration, could potentially demonstrate higher ADC values than LMSs [34]. Enhancement characteristics of leiomyomas are variable, with highly cellular leiomyomas often demonstrating marked early contrast enhancement. On the other hand, degenerated leiomyomas tend to show faint or irregular enhancement [64]. As a unifying feature however, non-treated leiomyomas usually lack areas of central contrast non-enhancement (necrosis) [29,64].

By comparison, LMSs usually present as solitary heterogeneous and poorly demarcated masses [34]. While their size can be variable, LMSs $\geq$ 10 cm have been found to be associated with a worse prognosis [68]. Their appearance on T1-weighted images is variable. They may show low or intermediate signal intensity like leiomyomas, but frequently demonstrate areas of high signal intensity on T1-weighted images, corresponding to hemorrhage or necrosis, therefore favouring malignancy [64]. LMSs show intermediate to high signal on T2-weighted images along with low ADC values, ranging from 0.79 ± 0.21 [SD] $\times 10^{-3}$ mm^2/s to 1.17 ± 0.15 [SD] $\times 10^{-3}$ mm^2/s; despite partial overlap, reported LMS ADC values can be lower relative to degenerated leiomyomas (1.17 ± 0.17 [SD] 10^{-3} mm^2/s to 1.7 ± 0.11 [SD] 10^{-3} mm^2/s) [9,27,32,34]. After intravenous administration of gadolinium-based contrast agents, they tend to enhance early and heterogeneously, often demonstrating non-enhancing areas of central necrosis [9,29].

The problem of overlap on MRI sequences

T1-weighted sequences

There can be marked overlap between certain imaging features, notably increased signal intensity on T1-weighted sequences, which can be seen in both leiomyoma and LMS, but due to different etiologies. Areas of high signal in a myometrial lesion on T1-weighted images may be due to intralesional fat, as seen in benign lipoleiomyomas. They might also represent red degeneration, resulting from hemorrhagic infarction in the context of pregnancy or

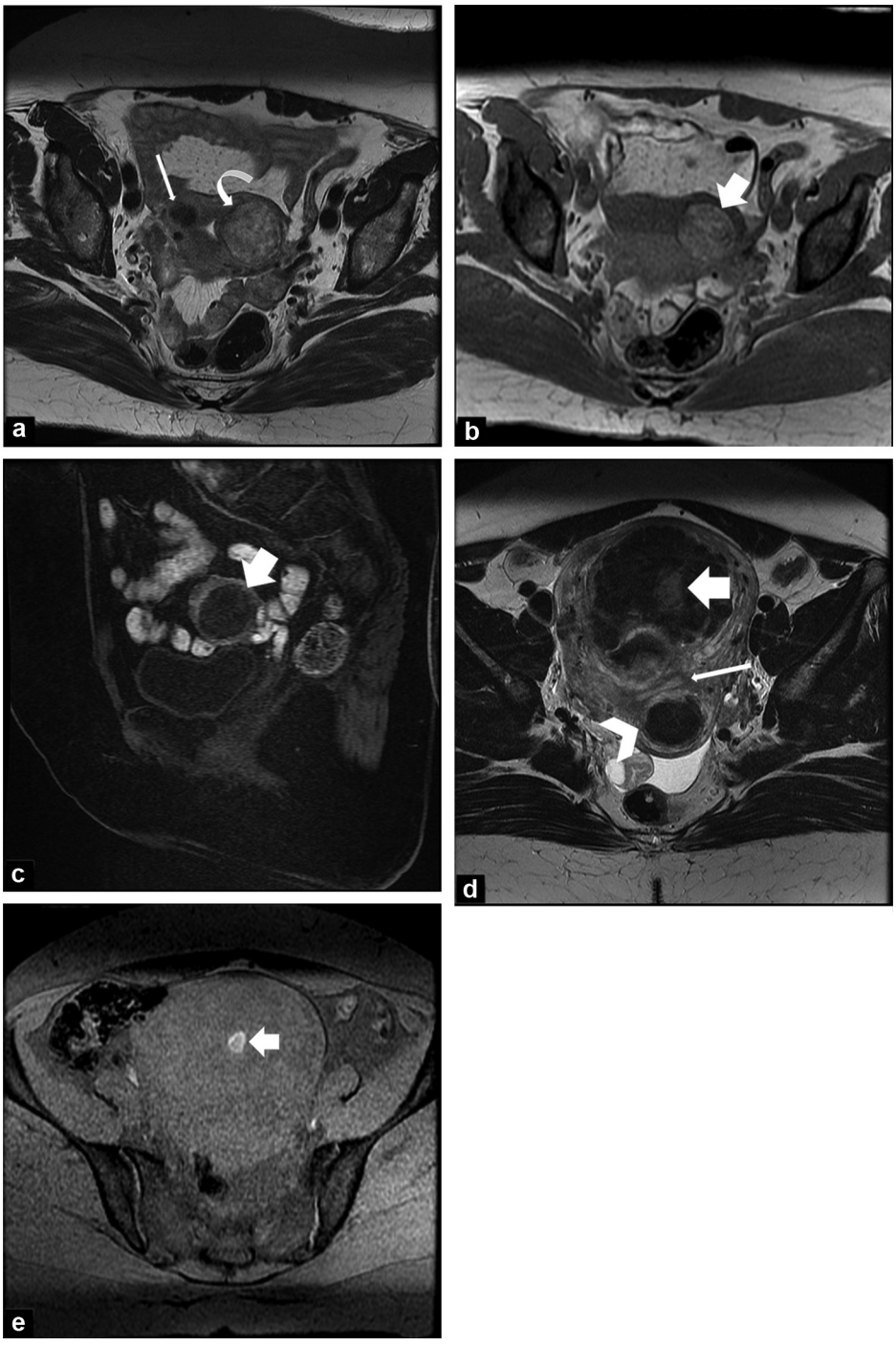

Figure 1. Role of T1-weighted precontrast sequences in differentiating the presence of intralesional fat and hemorrhagic components. a and b: 79-year-old woman with a well-defined rounded intramural lesion in the uterus, heterogeneously hyperintense on T2-weighted imaging (curved arrow, a) and with extensive fat content, as demonstrated by the T1-weighted in-phase (arrows, b) and T1-weighted fat suppressed precontrast images (arrows, c). A typical small intramural leiomyoma with low signal on T2-weighted imaging is also noted on the right (thin arrow, a). Patient underwent hysterectomy with final diagnosis of benign lipoleiomyoma. d and e: 45-year-old woman with a large leiomyoma in the anterior portion of the uterine body, showing diffuse low signal intensity on T2-weighted imaging (due to its increased proportion of smooth muscle content). It is also characterized by a focal central component demonstrating intermediate signal on T2-weighted imaging and high signal intensity on T1-weighted fat suppressed imaging, in keeping with intralesional hemorrhage or red degeneration (arrows, d and e). A typical intramural leiomyoma with low signal on T2-weighted imaging (arrowhead, d) is also noted posterior to the endometrium (thin white arrow, d).

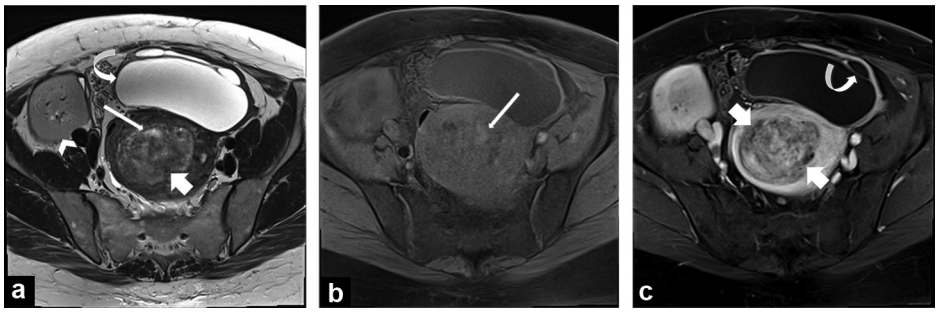

Figure 2. A 46-year-old woman with uterine leiomyoma with myxoid degeneration. a—c: 46-year-old woman with history of breast cancer and previous kidney transplant in the right lower quadrant (arrowhead, a). Axial MR images show the presence of a well-defined intramural uterine lesion in the fundus (thin arrows, a—c), characterized by heterogeneous signal on T2-weighted imaging mixed low/intermediate to high. A few slightly high signal intensity components are noted on the T1-weighted fat suppressed precontrast sequence (thin arrow, b). The lesion also shows tiny scattered areas of non-enhancement (<50%) (white arrows, c). The lesion has remained stable in size over 3 years of follow-up, along with two other dominant uterine leiomyomas (not shown). A lobulated non-enhancing tubular structure with a few internal septations is also noted in the left anterior pelvis, in keeping with a hydrosalpinx (curved arrows, a and c).

oral contraceptives, as usually seen in leiomyomas (Fig. 1) [69,70]. On the other hand, areas of high signal on T1-weighted images in LMS are often due to hemorrhage or necrosis [64]. Ideal assessment of signal characteristics on T1-weighted images should therefore be made with fat-saturated T1-weighted images. Additionally, subtracted contrast-enhanced sequences are critical and will differentiate hemorrhage from enhancing tissues in the setting of high signal areas on unenhanced T1-weighted images [64]. On the basis of these findings, high signal intensity involving nearly the entire lesion would favor leiomyoma; in contrast small heterogenous focal/multifocal areas of increased signal intensity on T1-weighted images may be attributable to focal hemorrhage or necrosis in the context of LMS if other aggressive features are associated.

T2-weighted sequences

Cellular atypia and high mitotic rates found in LMS cannot be directly assessed on MR imaging. However, the signal intensity on T2-weighted images, which is an imaging biomarker of tissue cellularity, may help in evaluating these tissue features [64,66]. Based on this principle, tumors with high cellularity (such as uterine LMS) and areas of necrosis would demonstrate increased signal on T2-weighted images. Despite somewhat conflicting opinions in the literature about the usefulness of simple T2 characteristics in the differentiation of LMS from leiomyoma [62], recent reviews have shown a significantly higher signal on T2-weighted images in LMSs in comparison to benign leiomyomas, which generally demonstrate homogenously low signal on T2-weighted images [3]. However, cystic and myxoid degeneration often show high signal on T2-weighted images, similar to large degenerative leiomyoma [71]. This therefore limits the predictive value of these criteria in individual patients (Fig. 2) and review of other MRI features is critical to aid in diagnosis (Fig. 6) [3,64,66].

DWI sequences

morphologic sequences, DWI has also been investigated as an adjunct to aid in the imaging diagnosis of LMSs [34]. Along with its visual qualitative analysis, DWI also allows for the quantitative measurement of the ADC values on the corresponding derived maps. These values vary based on the cellular density as a function of the nucleus-to-cytoplasm ratio [72,73]. Ordinary leiomyomas demonstrate low signal on DWI because of their corresponding low signal from hyalinized collagen on T2-weighted images, a so-called ''T2 blackout effect'' [74]. In a retrospective study of 5 LMSs and 51 leiomyomas, Tamai et al. found that all imaged uterine sarcomas demonstrated high signal intensity using high b-value DWI with corresponding decreased ADC value (1.17 ± 0.15 [SD] $\times 10^{-3}$ mm^2/s) in comparison to the myometrium. These findings are potentially attributable to the restricted motion of water molecules resulting from the increased cellularity, as typically found in malignant tumors [34]. However, the same study found that LMSs and highly cellular leiomyomas share overlapping ADC values (1.17 ± 0.15 [SD] $\times 10^{-3}$ mm^2/s and 1.19 ± 0.18 [SD] $\times 10^{-3}$ mm^2/s, respectively) [34]. In the literature, the reported ADC values for LMSs range from 0.79 ± 0.21 [SD] 10^{-3} mm^2/s to 1.17 ± 0.15 [SD] $\times 10^{-3}$ mm^2/s, while those for ordinary leiomyomas range from 0.88 ± 0.27 [SD] $\times 10^{-3}$ mm^2/s to 1.40 ± 0.31 [SD] $\times 10^{-3}$ mm^2/s [29,32—34,71]. Given the potential overlap between ranges, DWI and ADC alone are often not helpful in differentiating cellular leiomyoma from LMS and combination imaging with signal characteristics on T1- and T2-weighted images remains mandatory (Figs. 3 and 6).

Combination of MRI imaging features

To improve diagnostic accuracy and help address overlapping features, several authors have proposed combining multiple MRI features along with potential decision algorithms. Kaganov et al. have shown that there is a statistically significant relationship between increased signal intensity on T1-weighted images and higher risk of LMS [3]. This accordingly may favor a potential decision tree where presence of intralesional areas with high signal intensity on T1-weighted images would lead to subsequent evaluation of signal characteristics on T2-weighted images [3]. Tanaka et al. in a retrospective study of 9 LMSs and 12 leiomyomas reported

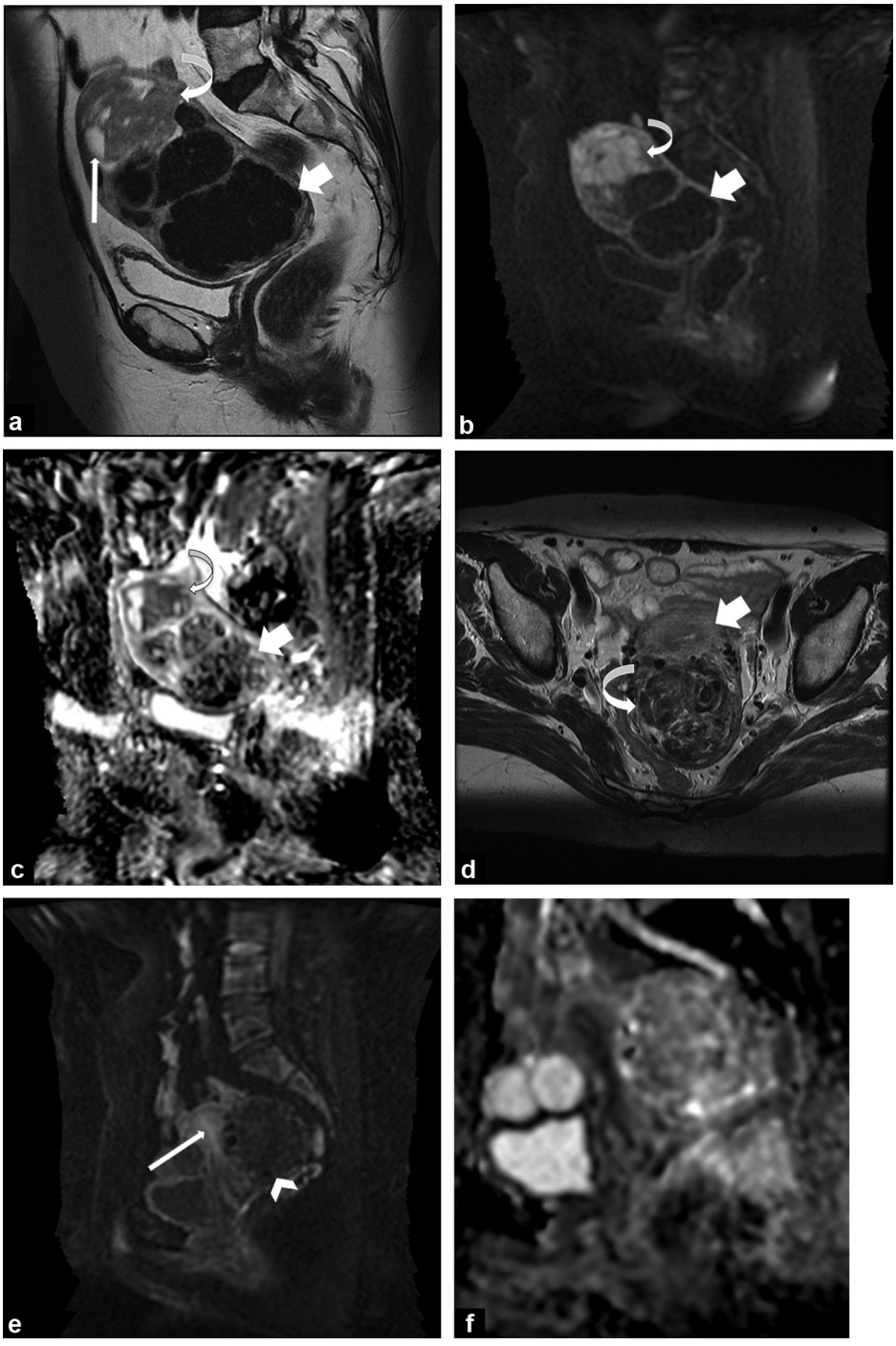

Figure 3. DWI and apparent diffusion coefficient (ADC) maps in leiomyosarcomas, typical and degenerated leiomyomas. a—c: 70-year-old woman with a malignant leiomyosarcoma in the uterine fundus (curved arrows, a—c). The leiomyosarcoma demonstrates intermediate signal intensity on T2-weighted imaging, with eccentric necrotic changes (thin arrow, a) and high signal intensity on b_{1000} diffusion-weighted imaging (b). The corresponding calculated apparent diffusion coefficient value is 873×10^{-3} mm/s (c). There are also several benign leiomyomas showing low signal on T2-weighted imaging (white arrows, a—c) and on diffusion-weighted imaging (b), with a corresponding ADC value of $796 \times 10 - 3$ mm/s (c). d—f: 67 year-old woman with a large intramural mass in the posterior uterine body. It shows heterogeneous low signal intensity (curved arrow, d) on T2-weighted imaging in comparison to the outer myometrium (arrow, d) and no restriction on b_{1000} diffusion-weighted imaging (arrowhead, e), which is defined in comparison to the intermediate signal intensity of the adjacent endometrium (thin arrow, e). The corresponding apparent diffusion coefficient value is 1661.73×10^{-3} mm/s (f). The patient underwent a total hysterectomy with a final diagnosis of markedly vascular atypical leiomyoma, characterized by extensive hyalinization and recent focal infarction secondary to thrombosis.

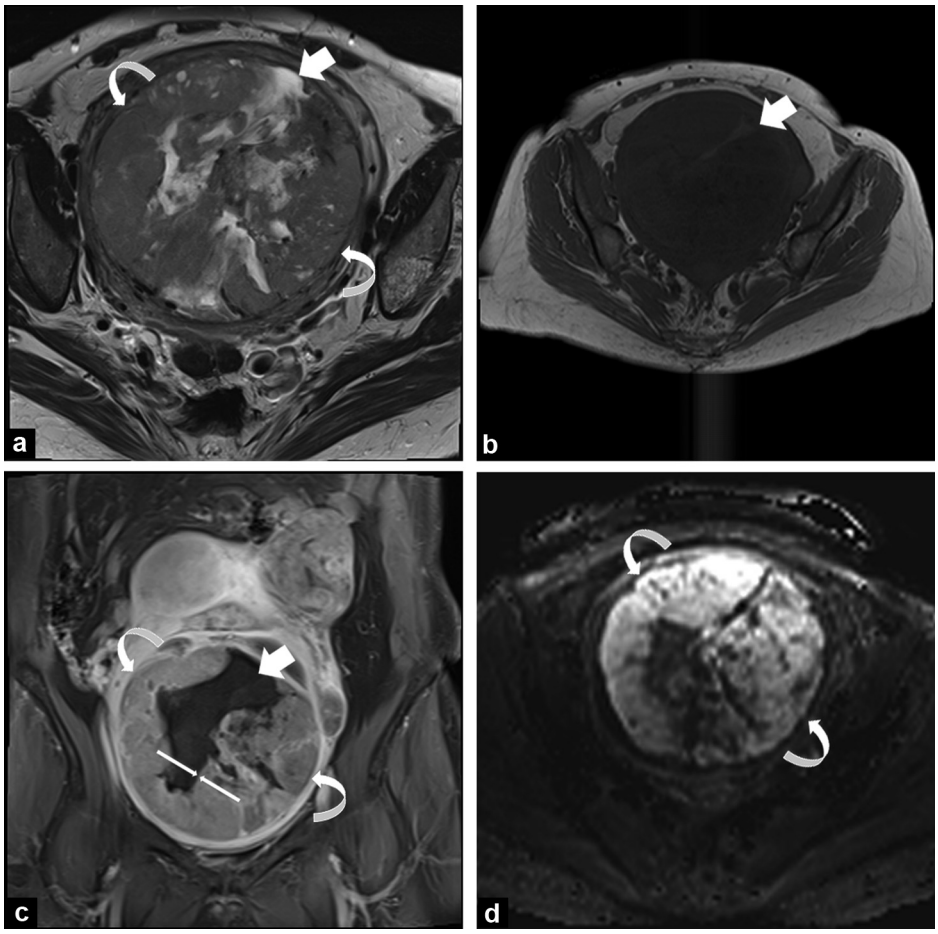

Figure 4. Leiomyosarcoma necrosis and non-enhancement. A 72-year-old woman with multiple leiomyomas and a large mass in the lower ventral uterine segment. The lesion shows internal hemorrhage and necrosis, corresponding to non-enhancing areas with high signal intensity on both T1- and T2-weighted imaging (large arrows, a—c). The dominant solid components show intermediate signal on T2-weighted imaging and high signal intensity on diffusion-weighted imaging (b_{1000}), which correlate to a high level of cellularity; these components also avidly enhance after gadolinium-chelate injection (curved arrows, a—c). There is an abrupt transitional zone between viable/enhancing cells and areas of necrosis, typical of leiomyosarcoma (thin arrows, c). The mass is confined to the uterus.

that the combination of the three following imaging features achieved a 73% sensitivity in diagnosing LMSs and STUMPs:

- more than 50% of the lesion demonstrating high signal on T2-weighted images;
- presence of internal focal areas of high signal intensity on T1-weighted sequences and;
- non-enhancing focal areas [62,64].

Given the very low prevalence of these tumors and therefore inherently high negative predictive value (NPV), specificity is much less important than sensitivity in this particular clinical context. Cornfeld et al., in a study that evaluated 4 LMSs and 17 leiomyomas, were only able to achieve a 17% sensitivity applying these criteria [62]. They reported instead that the presence of ill-defined margins achieved a sensitivity and specificity of 56% and 88%, respectively [62]. Additionally, they also noted that reader gestalt showed sensitivities ranging from 44% to 56%, with a 94% specificity [62]. Given that the readers in their study had extensive pelvic MRI interpretation experience (10 and 20 years, respectively), this may indicate that these results cannot be reliably reproduced for less subspecialized readers [62].

While rapid growth, usually defined as an increase in size of the uterus by 6 gestational weeks over 1 year, has been thought to favor a LMS over a leiomyoma, this is not a reliable finding. Parker at al. have shown in a retrospective study of 371 patients that only 0.27% of women operated for ''rapidly growing'' leiomyomas had a final diagnosis of uterine LMS [61,75]. Thomassin-Naggara et al. developed a multivariate model combining ADC values, b_{1000} signal intensity and characteristics on T2-weighted images to reach an overall accuracy of 92.4%, for the diagnosis of uterine sarcomas. Their retrospective study was not restricted to LMSs and included 25 malignant mesenchymal uterine tumors and 26 leiomyomas [21]. Their model takes into account the benign fibrous component of ordinary leiomyomas by using their corresponding low signal intensity on T2-weighted images. This is done in combination with the ability of high signal intensity on b_{1000} and corresponding low ADC values to demonstrate high cellularity, thus improving the ability to differentiate malignant tumors from equivocal benign but highly cellular leiomyomas.

More recently, a prospective study of 6 LMSs and 25 leiomyomas showed that the presence of hyperintensity on long b-value DWI alone did not improve the differentiation

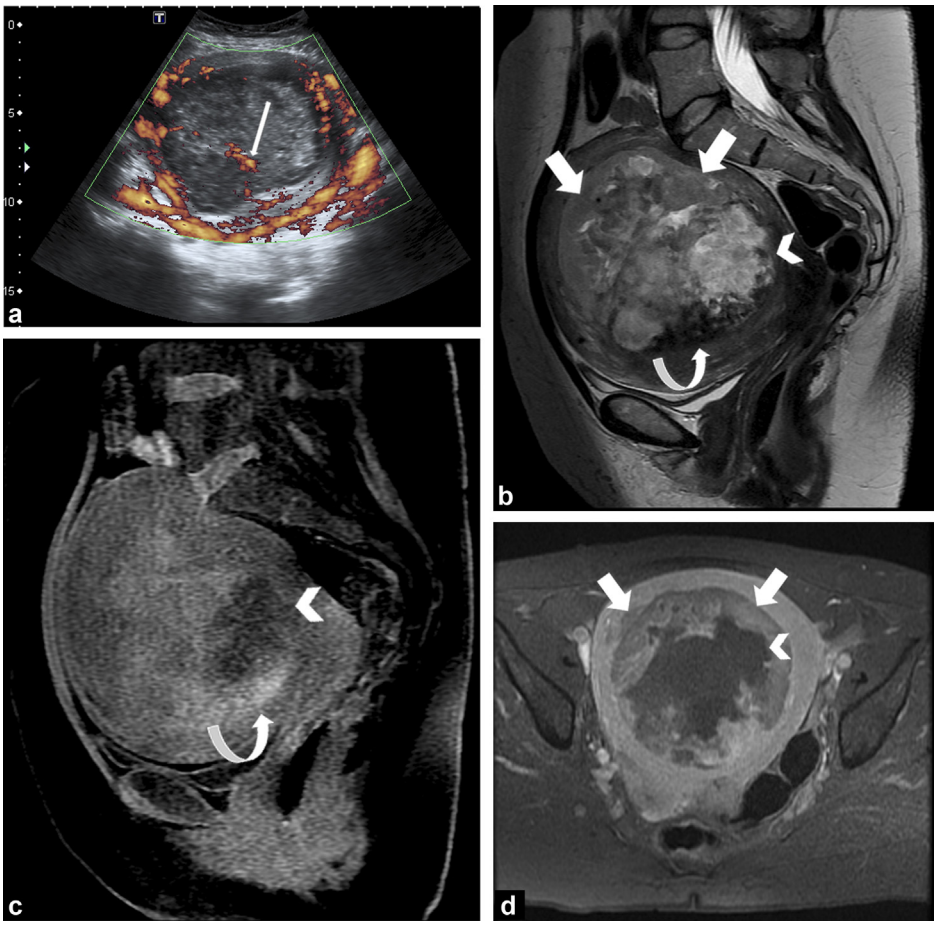

Figure 5. Necrosis, hemorrhage and solid components of a malignant leiomyosarcoma. A 51-year-old woman with a large uterine mass discovered during an ultrasound (a) performed for excessive vaginal bleeding. Doppler ultrasound shows increased vascularity within the mass (thin arrow, a). Multiparametric MRI (b–d) reveals a single heterogeneous intramural uterine mass with nodular borders. It shows solid, mainly peripheral, enhancing components with areas of tongue-like projections within the right anterior edges of the adjacent myometrium (arrows, b and d). The mass is also characterized by extensive necrotic changes (intermediate/high signal on T2-weighted imaging, low signal on T1-weighted imaging; arrowheads, b and c) and hemorrhagic components (low signal on T2- and intermediate/high signal on T1-weighted images; curved arrows, b and c). Both the necrotic changes and hemorrhagic components correspond to a central large non-enhancing area within the lesion (arrowhead, d). Biopsy confirmed a leiomyosarcoma of the uterus; at the time of diagnosis, the patient also had multiple liver, renal, lung and spinal metastatic lesions (not shown).

between LMSs and benign leiomyomas, only reaching an 52% accuracy and 36% specificity [29]. This study showed that adding an ADC cut-off value < 1.08×10^{-3} mm^2/s determined by posthoc analysis increased the overall accuracy of DWI to 88% [29]. However, the recommended ADC cut-off value for differentiating LMSs from leiomyomas varies between studies depending on whether b_{1000} signal intensities are included in the proposed models [21,33]. In the same study, the addition of contrast-enhanced MRI sequences further improved the diagnostic accuracy to 94%, with a sensitivity of 88% and a specificity of 96%. Also, the addition of contrast-enhanced sequences improved reader agreement ($\kappa = 0.921$) in comparison to DWI alone ($\kappa = 0.847$) [29]. The underlying principle behind the usefulness of contrast-enhanced MRI lies in the abrupt transitional zone from viable cells to necrotic cells lacking hyalinized tissue, termed coagulative necrosis (Figs. 4 and 5) [61,76]. Coagulative necrosis, frequently noted in LMSs, presents as an area of central non-enhancement on MRI, as opposed to the scattered areas of non-enhancement that may be encountered in leiomyomas with degeneration due to their inherent interlacing pattern of viable and degenerative cells (Fig. 2) [29]. While a useful predictor of malignancy, the presence of non-enhancing central areas observed on post-contrast images is not infallible and may also be seen in benign leiomyomas with extensive vascular infarction [29,62]. Lakhman et al. have also confirmed the value of a multivariate model for the diagnosis of LMS by combining three or more of the following imaging features: nodular borders, hemorrhage, ''T2 dark'' signal areas and lack of central enhancement, achieving a sensitivity and specificity of 100% and 95%, respectively [4].

Recent developments

In the wake of recent computer advancements, TA has also been investigated as an adjunct for the diagnosis of LMS on MRI. TA allows computerized conversion of local variations in image pixel intensities into quantifiable outputs [4]. While TA has been frequently investigated in the diagnosis

Table 3 Summary of landmark MRI studies.

Author	Year	Study design	LMS lesions (*n*)	Benign lesions (*n*)	Results (main imaging features in favor of LMS)
Tanaka et al. [64]	2004	Retrospective	9	12	>50% high signal area on T2WI, small high-signal areas on T1WI with unenhanced pockets
Tamai et al. [34]	2007	Retrospective	5	51	High signal intensity on DWI Mean ADC 1.17 ± 0.15 (SD) $\times 10^{-3}$ mm^2/s
Cornfeld et al. [62]	2010	Retrospective	4	17	No statistically significant morphological features Ill-defined margins ($P = 0.06$) Reader gestalt ($P = 0.02$)
Thomassin-Naggara et al. [21]	2013	Retrospective	3	26	Combination of: age > 44.8 years; high b_{1000} signal intensity; intermediate signal on T2WI; ADC cut-off < 1.23×10^{-3} mm^2/s (mean sarcoma ADC 0.97 ± 0.15 [SD] $\times 10^{-3}$ mm^2/s)
Lin et al. [29]	2016	Prospective	6	25	Central non-enhancement on contrast-enhanced MRI High signal intensity on DWI + ADC cut-off < 1.08×10^{-3} mm^2/s (mean sarcoma ADC 1.02 ± 0.35 [SD] $\times 10^{-3}$ mm^2/s)
Lakhman et al. [4]	2017	Retrospective	19	22	Nodular borders, hemorrhage, dark areas on T2WI, central non-enhancement ($P \leq 0.0001$) (Best when ≥ 3 of the above) Greater textural heterogeneity (higher intensity image-based and Gabor edge image-based contrast, lower energy, lower homogeneity, lower kurtosis)
Gerges et al. [22]	2018	Retrospective	17	51	T2WI histogram metric mean below the 50th percentile, best below the 10th percentile ($Mean_{0-10}$)

LMS: leiomyosarcoma; T1WI: T1-weighted images; T2WI: T2-weighted images.

of prostate, head and neck and ovarian cancer, very few studies have assessed its usefulness in the diagnosis of LMS [30,77,78]. Lakhman et al. have shown in a retrospective study of 41 patients, that 16/21 extracted texture features were significantly different between 19 LMSs and 22 atypical leiomyomas. In particular, LMSs demonstrated greater overall textural heterogeneity suggested by higher intensity image-based and Gabor edge image-based contrast, lower energy, lower kurtosis and higher standard deviation [4]. It is important to note that the combination of both intensity-based and Gabor edge image-based texture features yielded higher accuracy (75%) in comparison to Gabor edge image-based features alone (58%) [4]. As a proof of concept, Lakhman et al. only applied TA to T2-weighted images and did not fully assess its value independently from conventionally established MRI features reported in the literature [4,22]. More recently, Gerges et al. have also investigated the utility of TA for the diagnosis of LMS on multiple MRI sequences in a retrospective study with 17 LMSs and 51 leiomyomas [22]. They determined that histogram metrics from TA were most useful on T2-weighted images and least helpful on ADC maps, with the most useful metric derived from the actual signal intensity rather than the metrics of lesion texture [22]. More specifically T2 histogram means below the 50th percentile achieved an area under the curve (AUC) of up to 0.875. These results reflect the ability of the metrics to accurately identify lesion subregions with very low signal on T2-weighted images, which is a characteristic that strongly favors a leiomyoma given their higher smooth muscle content versus LMS [22]. Additionally, to confirm what has been previously reported [4,21], Gerges et al. have reiterated that patient age over 44 years, whether as an independent variable or combined with a multivariable model, strongly favored the diagnosis of a LMS [22].

While the current literature has attempted to clarify the ability of MRI to differentiate LMSs from leiomyomas, most

Table 4 Summary of the main MRI and PET/CT characteristics favoring either leiomyoma or leiomyosarcoma.

	Leiomyoma	Leiomyosarcoma
Patient age	Premenopausal (<44 years)	Peri/postmenopausal (>44 years)
Size	Variable	Variable (>10 cm, associated with poorer prognosis) [70]
Margins	Well-defined	Irregular and ill-defined, often nodular and with invasion of adjacent structures
Signal on T1WI	Low to intermediate High for fat content or hemorrhage	Heterogenous and low High for hemorrhage from necrosis
Signal on T2WI	Generally, homogenous low signal Intermediate/high in myxoid/cystic degeneration	Intermediate to high signal Signal on T2WI
DWI and ADC signal	Low DWI, low ADC SI: ordinary Low DWI, high ADC SI: highly cellular Low DWI, high ADC SI: degenerated	Generally high DWI and low ADC SI
ADC values (10^{-3} mm^2/s) [29,32–34]	0.88 ± 0.27 to 1.40 ± 0.31: ordinary 1.13 ± 0.18 to 1.43 ± 0.58: highly cellular 1.17 ± 0.17 to 1.7 ± 0.11: degenerated	0.79 ± 0.21 (SD) to 1.17 ± 0.1 (SD) (overlap with leiomyomas)
Contrast-enhanced MRI	Variable Can show scattered areas of contrast non-enhancement in hyaline degeneration Hypercellular types will enhance avidly	Early heterogenous enhancement with central areas of contrast non-enhancement
Texture analysis		Greater textural heterogeneity (higher intensity image-based and Gabor edge image-based contrast, lower energy, lower homogeneity, lower kurtosis) T2WI histogram means below the 50th percentile
PET/CT	SUVmax < 7.5	SUVmax > 7.5

T1WI: T1-weighted images; T2WI: T2-weighted images.

studies consist of case reports and retrospective studies, with very few prospective analyses [29]. Another unavoidable limitation common to the literature is undoubtedly the rarity of LMS, which inherently limits the sample size, statistical power and external validity of these findings (Table 3) [62].

To summarize, for accurate diagnosis of LMS, the evidence in the current MRI literature seems to favor ill-defined margins, high DWI on b1000 images and low ADC signal along with lack of central contrast enhancement (Table 4) [4,21,29,33,34,64]. The presence of corresponding high signal intensity on both T1- and T2-weighted imaging can also favour the diagnosis of LMS through the use of a systematic decision tree [3]. While relatively new in the evaluation of LMS, texture analysis has also shown promising initial results by noting increased texture heterogeneity and low percentile histogram means on T2-weighted sequences for LMS (Table 4) [4,22]. Because the integration of individual imaging features can often prove difficult in the differentiation of LMS from leiomyoma, we have attempted to provide a diagnostic flowchart to help direct radiologists based on the presence of selected salient MRI features (Fig. 6).

FDG PET/CT

While CT alone is not particularly helpful for the differentiation of leiomyomas from LMSs, it has shown utility in combination with 18F-Fludeoxyglucose (18F-FDG)-PET in the context of indeterminate myometrial lesions on MRI [79,80]. It is thought that malignant tumors experience upregulation of glucose transporter genes (GLUTs) either due to increase of normal cellular enzymes or synthesis of new transporters after transformation due to oncogenes [81,82]. Based on this hypothesis, greater 18F-FDG uptake of LMS would be expected in comparison to leiomyomas due to their increased metabolic rate and glycolysis. There are few studies on this specific topic, however a study by Umesaki et al. has shown 100% sensitivity of 18F-FDG PET in the diagnosis of uterine sarcoma vs. leiomyoma with a positive standardized uptake value (SUV) cut-off value of 2.5 [83]. The mean standardized uptake value (SUV) of sarcomas was 4.5 ± 1.3 (SD), with LMS demonstrating elevated SUV values between 3 and 4 [83]. However, only five patients had uterine sarcoma, with only 3 of them having LMS. While 18F-FDG uptake in leiomyoma is generally low with reported SUV_{max} of up to 1.74 ± 0.50 (SD), Chura et al. have

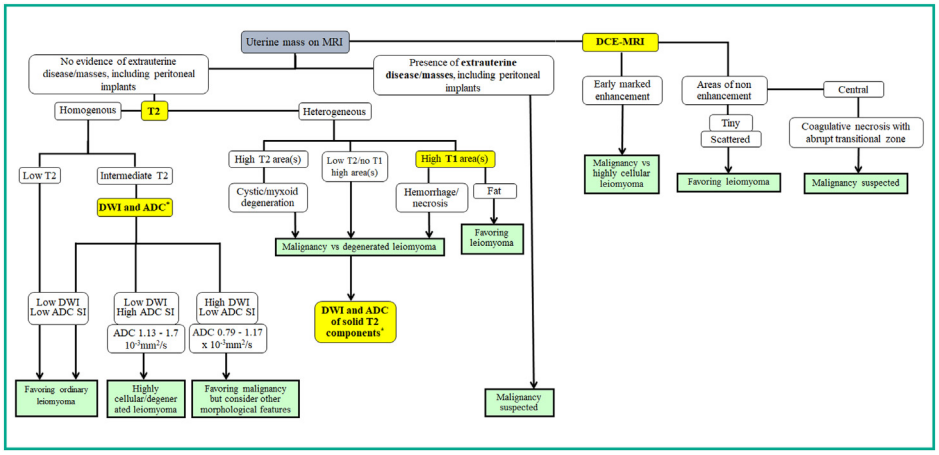

Figure 6. Diagnostic algorithm for MRI differentiation of uterine leiomyomas and leiomyosarcomas. The signal intensity of the endometrium is generally the standard of reference against which the diffusion-weighted imaging (DWI) signal intensity (low/intermediate/high) of a uterine lesion is defined. For T2-weighted sequences, the lesion is generally considered hyperintense in comparison to the signal intensity of the outer myometrium. The presence or absence of any extrauterine disease/mass refers to what is covered by the field of view of the pelvic MRI. (ADC: apparent diffusion coefficient; SI: signal intensity).

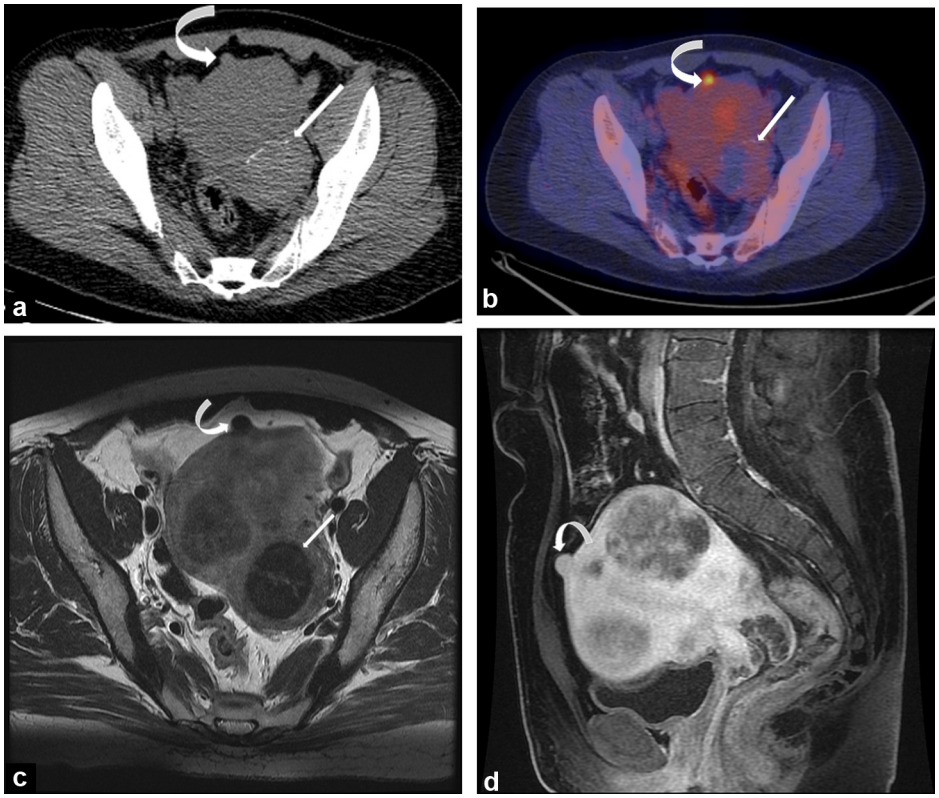

Figure 7. 18F-FDG PET/CT images and SUV values of a benign leiomyoma and leiomyosarcoma. A 44-year-old woman with malignant phyllodes breast tumor. On the staging PET scan, abnormal FDG uptake was found (SUV 5.4) in a small, exophytic lesion in the uterine fundus (curved arrows, a and b); a partially calcified lesion without any uptake is also noted within the posterior aspect of the uterus (thin arrows a and b). A dedicated pelvic MRI showed a bulky uterus with multiple leiomyomas, one of which demonstrated typical low signal intensity on T2-weighted imaging (thin arrow, c), corresponding to the partially calcified lesion observed on the 18F-FDG PET/CT scan. A small anterior fundal subserosal exophytic leiomyoma, demonstrating homogeneous post-contrast enhancement and typical low signal intensity on T2-weighted imaging, is also noted and corresponds to the source of radiotracer uptake on PET scan (curved arrows, c and d). The lesion has remained stable on imaging over a period of 4 years, confirming its benign nature.

noted that it can sometimes be elevated in cases of cellular leiomyomas (SUV = 9.3) or even in ordinary leiomyomas (SUV = 16), if they happen to be particularly vascular, thus leading to false-positive diagnoses (Fig. 7) [84,85]. Overall, no uptake on FDG PET will help out rule out a LMS, but a positive result is not as helpful since it is not necessarily diagnostic for LMS. More recently, Kusonoki et al. have reported that a cut-off SUVmax value > 7.5 was able to exclude leiomyoma with an 81% sensitivity and a 100% specificity (n = 15 uterine sarcomas and 19 leiomyomas), thus decreasing the false-positive rate [79]. Additionally, 3'-deoxy-3'-[^{18}F]-flurothymidine (18F-FLT) has also been investigated as an alternative radiotracer in the differentiation of uterine sarcomas from benign leiomyomas, showing better performance in comparison to 18F-FDG in terms of specificity (90 vs. 70%), PPV (83.9 vs. 62.5%) and accuracy (93.3 vs. 80%) [86]. While the number of patients was low with three LMSs and 10 leiomyomas, 18F-FLT-PET specifically showed low uptake in a leiomyoma that had high uptake on 18F-FDG PET, therefore this could potentially be used as a confirmatory adjunct in doubtful lesions [86].

In terms of initial staging, 18F-FDG PET/CT has shown excellent performance with a sensitivity, specificity and accuracy reaching up to 80, 100 and 91%, respectively. [87] 18F-FDG PET/CT is particularly helpful for detecting peritoneal metastases camouflaged between bowel loops, given its ability to outline their increased metabolic activity in comparison to CT alone, and for detecting distant metastasis (sensitivity up to 100% in some studies) [80,88,89]. However, 18F-FDG PET/CT appears somewhat limited for local pelvic and para-aortic lymph node staging, with a sensitivity of only 58%, although the number of studies on this specific area is currently limited [80,89]. Finally, 18F-FDG PET/CT has also proven highly useful for discriminating between true disease recurrence both in asymptomatic patients and in those with clinical suspicion of recurrent disease, reaching a sensitivity, specificity, accuracy, PPV and NPV of 87.5—92.9%, 95.5—100%, 93.3—94.4%, 87.5—100% and 80—95.5% respectively [80,87,90].

The value of SUV_{max} on preoperative 18F-FDG PET/CT is a powerful prognostic factor for overall and disease-free survival, outperforming more conventional variables such as FIGO stage or tumor size [91]. Specifically, in a series of 19 patients, Park et al. have ascertained more favorable outcomes for patients with tumors exhibiting SUV_{max} < 23.95. [91].

Staging

LMSs tend to spread systematically from the myometrium through the pelvic blood vessels and lymphatics into the adjacent pelvic organs, abdomen and lungs [59]. Precise staging with the 2009 FIGO classification (Table 1), which is now specific to uterine LMS, should be performed to ensure an optimal management [10,92]. A detailed discussion of the role of imaging in staging LMS is however beyond the scope of this manuscript. However, it is important to note that because of the difficulty in the preoperative diagnosis of LMS, many patients initially undergo surgery for presumed benign leiomyomas detected on US. These patients are typically treated by general gynecologists without advanced imaging evaluation or frozen tissue preservation [93]. As a result, this often leads to incomplete surgical staging and a suboptimal primary surgical resection with poorer patient outcomes [3].

Conclusion

Despite current state of the art advances in the imaging differentiation of LMS from atypical leiomyomas, there remains a certain lack of consensus regarding the individual usefulness of MRI features. Through our review of the current diagnostic imaging literature on the subject, we have attempted to summarize and highlight the principal MRI imaging features felt to aid in favoring a diagnosis of LMS over leiomyoma (Table 3). Because assessing the value of individual imaging features may often prove challenging in the context of obtaining a clear diagnosis, we have also attempted to provide some guidance through the use of a diagnostic algorithm combining multiple imaging features (Fig. 6). Further prospective studies with larger populations of interest, using multivariate models with computed image analysis and machine learning could potentially further improve consensus on the ability of MRI to accurately differentiate LMSs from atypical leiomyomas.

Funding

This work did not receive any grant from funding agencies in the public, commercial, or not-for-profit sectors.

Author contributions

All authors attest that they meet the current International Committee of Medical Journal Editors (ICMJE) criteria for Authorship.

Simon Sun: conceptualization, methodology, validation, formal analysis, investigation, resources, data curation, writing — original draft, writing — review and editing, visualization and project administration.

Pietro A Bonaffini: conceptualization, methodology, validation, formal analysis, investigation, resources, data curation, writing — original draft, writing — review and editing and visualization.

Stephanie Nougaret: conceptualization, methodology, validation, formal analysis, investigation, data curation, writing — review and editing and supervision.

Laure Fournier: conceptualization, methodology, validation, writing — review and editing supervision.

Anthony Dohan: conceptualization, methodology, writing — review and editing and supervision.

Jaron Chong: conceptualization, methodology, writing — review and editing and supervision.

Jan Smith: conceptualization, methodology, writing — review and editing and supervision.

Helen Addley: conceptualization, methodology, writing — review and editing and supervision.

Caroline Reinhold: conceptualization, methodology, validation, formal analysis, data curation, resources, writing

— review and editing, visualization, supervision and project administration.

Disclosure of interest

The authors declare that they have no competing interest.

References

[1] Pavone D, Clemenza S, Sorbi F, Fambrini M, Petraglia F. Epidemiology and risk factors of uterine fibroids. Best Pract Res Clin Obstet Gynaecol 2018;46:3—11.

[2] Parker WH. Etiology, symptomatology, and diagnosis of uterine myomas. Fertil Steril 2007;87:725—36.

[3] Kaganov H, Ades A, Fraser DS. Preoperative magnetic resonance imaging diagnostic features of uterine leiomyosarcomas: a systematic review. Int J Technol Assess Health Care 2018;34:172—9.

[4] Lakhman Y, Veeraraghavan H, Chaim J, Feier D, Goldman DA, Moskowitz CS, et al. Differentiation of uterine leiomyosarcoma from atypical leiomyoma: diagnostic accuracy of qualitative MR imaging features and feasibility of texture analysis. Eur Radiol 2017;27:2903—15.

[5] Vilos GA, Allaire C, Laberge P-Y, Leyland N, Vilos AG, Murji A, et al. The management of uterine leiomyomas. J Obstet Gynaecol Can 2015;37:157—78.

[6] ACOG. Uterine leiomyomata. Int J Gynaecol Obstet 1994;46:73—82.

[7] del Carmen MG. Uterine leiomyosarcoma. In: del Carmen MG, Young RH, Schorge JO, Birrer MJ, editors. Uncommon gynecologic cancers. 2014.

[8] Wu TI, Yen TC, Lai CH. Clinical presentation and diagnosis of uterine sarcoma, including imaging. Best Pract Res Clin Obstet Gynaecol 2011;25:681—9.

[9] Santos P, Cunha TM. Uterine sarcomas: clinical presentation and MRI features. Diagn Interv Radiol 2015;21:4—9.

[10] D'Angelo E, Prat J. Uterine sarcomas: a review. Gynecol Oncol 2010;116:131—9.

[11] Toro JR, Travis LB, Wu HJ, Zhu K, Fletcher CDM, Devesa SS. Incidence patterns of soft tissue sarcomas, regardless of primary site, in the surveillance, epidemiology and end results program, 1978—2001: an analysis of 26,758 cases. Intern J Cancer 2006;119:2922—30.

[12] Koivisto-Korander R, Martinsen JI, Weiderpass E, Leminen A, Pukkala E. Incidence of uterine leiomyosarcoma and endometrial stromal sarcoma in Nordic countries: results from nordcan and nocca databases. Maturitas 2012;72:56—60.

[13] Pietzner K, Buttmann-Schweiger N, Sehouli J, Kraywinkel K. Incidence patterns and survival of gynecological sarcoma in Germany: analysis of population-based cancer registry data on 1066 women. Int J Gynecol Cancer 2018;28:134—8.

[14] Puliyath G, Nair MK. Endometrial stromal sarcoma: a review of the literature. Indian J Med Paediatr Oncol 2012;33:1—6.

[15] Mori KM, Abaid LN, Mendivil AA, Brown JV, Beck TL, Micha JP, et al. The incidence of occult malignancy following uterine morcellation: a ten-year single institution experience retrospective cohort study. Int J Surg 2018;53:239—42.

[16] Rodriguez AM, Asoglu MR, Sak ME, Tan A, Borahay MA, Kilic GS. Incidence of occult leiomyosarcoma in presumed morcellation cases: a database study. Eur J Obstet Gynecol Reprod Biol 2016;197:31.

[17] Sizzi O, Manganaro L, Rossetti A, Saldari M, Florio G, Loddo A, et al. Assessing the risk of laparoscopic morcellation of occult uterine sarcomas during hysterectomy and myomectomy: literature review and the ISGE recommendations. Eur J Obstet Gynecol Reprod Biol 2018;220:30—8.

[18] Marret H, Fritel X, Ouldamer L. Therapeutic management of uterine fibroid tumors: updated French guidelines. Eur J Obstet Gynecol Reprod Biol 2012;165:156.

[19] Littell RD, Tucker LY, Raine-Bennett T, Palen TE, Zaritsky E, Neugebauer R, et al. Adjuvant gemcitabine-docetaxel chemotherapy for stage I uterine leiomyosarcoma: trends and survival outcomes. Gynecol Oncol 2017;147:11—7.

[20] Major FJ, Blessing JA, Silverberg SG, Morrow CP, Creasman WT, Currie JL, et al. Prognostic factors in early-stage uterine sarcoma: a Gynecologic Oncology Group Study. Cancer 1993;71:1702—9.

[21] Thomassin-Naggara I, Dechoux S, Bonneau C. How to differentiate benign from malignant myometrial tumours using MR imaging. Eur Radiol 2013;23:2306.

[22] Gerges L, Popiolek D, Rosenkrantz AB. Explorative investigation of whole-lesion histogram MRI metrics for differentiating uterine leiomyomas and leiomyosarcomas. AJR Am J Roentgenol 2018;210:1172—7.

[23] Brohl AS, Li L, Andikyan V, Običan SG, Cioffi A, Hao K, et al. Age-stratified risk of unexpected uterine sarcoma following surgery for presumed benign leiomyoma. Oncologist 2015;20:433—9.

[24] Kapp DS, Shin JY, Chan JK. Prognostic factors and survival in 1396 patients with uterine leiomyosarcomas. Cancer 2008;112:820—30.

[25] Nordal RR, Thoresen SØ. Uterine sarcomas in Norway 1956—1992: incidence, survival and mortality. Eur J Cancer 1997;33:907—11.

[26] Bogani G, Fucà G, Maltese G, Ditto A, Martinelli F, Signorelli M, et al. Efficacy of adjuvant chemotherapy in early stage uterine leiomyosarcoma: a systematic review and meta-analysis. Gynecol Oncol 2016;143:443—7.

[27] Li HM, Liu J, Qiang JW, Zhang H, Zhang GF, Ma F. Diffusion-weighted imaging for differentiating uterine leiomyosarcoma from degenerated leiomyoma. J Comput Assist Tomogr 2017;41:599.

[28] Skorstad M, Kent A, Lieng M. Preoperative evaluation in women with uterine leiomyosarcoma: a nationwide cohort study. Acta Obstet Gynecol Scand 2016;95:1228.

[29] Lin G, Yang LY, Huang YT. Comparison of the diagnostic accuracy of contrast-enhanced MRI and diffusion-weighted MRI in the differentiation between uterine leiomyosarcoma/smooth muscle tumor with uncertain malignant potential and benign leiomyoma. J Magn Reson Imaging 2016;43:333.

[30] Jansen JF, Lu Y, Gupta G. Texture analysis on parametric maps derived from dynamic contrast-enhanced magnetic resonance imaging in head and neck cancer. World J Radiol 2016;8:90.

[31] Gaetke-Udager K, McLean K, Sciallis AP, Alves T, Maturen KE, Mervak BM, et al. Diagnostic accuracy of ultrasound, contrast-enhanced CT, and conventional MRI for differentiating leiomyoma from leiomyosarcoma. Acad Radiol 2016;23:1290—7.

[32] Sato K, Yuasa N, Fujita M, Fukushima Y. Clinical application of diffusion-weighted imaging for preoperative differentiation between uterine leiomyoma and leiomyosarcoma. Am J Obstet Gynecol 2014;210 [368.e361].

[33] Namimoto T, Yamashita Y, Awai K, Nakaura T, Yanaga Y, Hirai T, et al. Combined use of T2-weighted and diffusion-weighted 3-T MR imaging for differentiating uterine sarcomas from benign leiomyomas. Eur Radiol 2009;19:2756.

[34] Tamai K, Koyama T, Saga T, Morisawa N, Fujimoto K, Mikami Y, et al. The utility of diffusion-weighted MR imaging for differentiating uterine sarcomas from benign leiomyomas. Eur Radiol 2008;18:723—30.

[35] Walker CL, Stewart EA. Uterine fibroids: the elephant in the room. Science 2005;308:1589—92.

[36] Evans HL, Chawla SP, Simpson C, Finn KP. Smooth muscle neoplasms of the uterus other than ordinary leiomyoma: a study of 46 cases, with emphasis on diagnostic criteria and prognostic factors. Cancer 1988;62:2239—47.
[37] Perrone TMD, Dehner LPMD. Prognostically favorable ''mitotically active'' smooth-muscle tumors of the uterus: a clinicopathologic study of ten cases. Am J Surg Pathol 1988;12:1—8.
[38] Gockley AA, Rauh-Hain JA, del Carmen MG. Uterine leiomyosarcoma: a review article. Int J Gynecol Cancer 2014;24:1538—42.
[39] Kurman RJ, Norris HJ. Mesenchymal tumors of the uterus VI. Epithelioid smooth muscle tumors including leiomyoblastoma and clear-cell leiomyoma: a clinical and pathologic analysis of 26 cases. Cancer 1976;37:1853—65.
[40] Lu B, Shi H, Zhang X. Myxoid leiomyosarcoma of the uterus: a clinicopathological and immunohistochemical study of 10 cases. Hum Pathol 2017;59:139—46.
[41] Ip PPC, Cheung ANY, Clement PB. Uterine smooth muscle tumors of uncertain malignant potential (stump): a clinicopathologic analysis of 16 cases. Am J Surg Pathol 2009;33:992—1005.
[42] Hernando E, Charytonowicz E, Dudas ME, Menendez S, Matushansky I, Mills J, et al. The AKT-MTOR pathway plays a critical role in the development of leiomyosarcomas. Nat Med 2007;13:748.
[43] Cuppens T, Tuyaerts S, Amant F. Potential therapeutic targets in uterine sarcomas. Sarcoma 2015;2015:243298.
[44] Tsuyoshi H, Yoshida Y. Molecular biomarkers for uterine leiomyosarcoma and endometrial stromal sarcoma. Cancer Sci 2018;109:1743—52.
[45] Farquhar CM, Steiner CA. Hysterectomy rates in the United States 1990—1997. Obstet Gynecol 2002;99:229—34.
[46] Sparic R, Mirkovic L, Malvasi A, Tinelli A. Epidemiology of uterine myomas: a review. Int J Fertil Steril 2016;9:424—35.
[47] Chiumente M, De Rosa M, Messori A, Proli EM. Burden of uterine fibroids in Italy: epidemiology, treatment outcomes, and consumption of health care resources in more than 5,000 women. Clinicoecon Outcomes Res 2017;9:525—35.
[48] Babacan A, Kizilaslan C, Gun I, Muhcu M, Mungen E, Atay V. CA 125 and other tumor markers in uterine leiomyomas and their association with lesion characteristics. Int J Clin Exp Med 2014;7:1078—83.
[49] Cho FN, Liu CB, Li JY, Chen SN, Yu KJ. Dramatic changes of CA 125 levels in a pregnant woman with a degenerated subserosal myoma. Taiwan J Obstet Gynecol 2012;51:117—8.
[50] Juang CM, Yen MS, Horng HC, Twu NF, Yu HC, Hsu WL. Potential role of preoperative serum CA 125 for the differential diagnosis between uterine leiomyoma and uterine leiomyosarcoma. Eur J Gynaecol Oncol 2006;27:370—4.
[51] Menczer J, Schreiber L, Berger E, Ben-Shem E, Golan A, Levy T. CA 125 expression in the tissue of uterine leiomyosarcoma. Isr Med Assoc J 2014;16:697—9.
[52] Woźniak A, Woźniak S. Ultrasonography of uterine leiomyomas. Prz Menopauzalny 2017;16:113—7.
[53] Rami A, Yifat O, Ofer M, Ami F, Ilan CMAM, et al. Uterine sarcomas versus leiomyomas: gray-scale and Doppler sonographic findings. J Clin Ultrasound 2005;33:10—3.
[54] Kurjak A, Kupesic S, Shalan H, Jukic S, Kosuta D, Ilijas M. Uterine sarcoma: a report of 10 cases studied by transvaginal color and pulsed Doppler sonography. Gynecol Oncol 1995;59:342.
[55] Caterina E, Elisabetta RM, Annalisa A, Concetta A, Beata S, Errico Z, et al. Can gray-scale and color Doppler sonography differentiate between uterine leiomyosarcoma and leiomyoma? J Clin Ultrasound 2007;35:449—57.
[56] Rha SE, Byun JY, Jung SE, Lee SL, Cho SM, Hwang SS, et al. CT and MRI of uterine sarcomas and their mimickers. AJR Am J Roentgenol 2003;181:1369—74.
[57] Roy C, Bierry G, Ghali SE, Buy X, Rossini A. Acute torsion of uterine leiomyoma: CT features. Abdom Imaging 2004;30:120—3.
[58] Ohgiya Y, Seino N, Miyamoto S, Takeyama N, Hatano K, Munechika J, et al. CT features for diagnosing acute torsion of uterine subserosal leiomyoma. Jpn J Radiol 2018;36:209—14.
[59] Qiu LL, Yu RS, Chen Y, Zhang Q. Sarcomas of abdominal organs: computed tomography and magnetic resonance imaging findings. Semin Ultrasound CT MR 2011;32:405—21.
[60] Tonolini M. Multidetector CT of expected findings and complications after hysterectomy. Insights Imaging 2018;9:369—83.
[61] Shah SH, Jagannathan JP, Krajewski K, O'Regan KN, George S, Ramaiya NH. Uterine sarcomas: then and now. AJR Am J Roentgenol 2012;199:213—23.
[62] Cornfeld D, Israel G, Martel M, Weinreb J, Schwartz P, McCarthy S. MRI appearance of mesenchymal tumors of the uterus. Eur J Radiol 2010;74:241—9.
[63] Kubik-Huch RA, Weston M, Nougaret S, Leonhardt H, Thomassin-Naggara I, Horta M, et al. European Society of Urogenital Radiology (ESUR) guidelines: MR imaging of leiomyomas. Eur Radiol 2018;28:3125—37.
[64] Tanaka YO, Nishida M, Tsunoda H, Okamoto Y, Yoshikawa H. Smooth muscle tumors of uncertain malignant potential and leiomyosarcomas of the uterus: MR findings. J Magn Reson Imaging 2004;20:998—1007.
[65] Togashi K, Ozasa H, Konishi I, Itoh H, Nishimura K, Fujisawa I, et al. Enlarged uterus: differentiation between adenomyosis and leiomyoma with MR imaging. Radiology 1989;171:531—4.
[66] Yamashita Y, Torashima M, Takahashi M, Tanaka N, Katabuchi H, Miyazaki K, et al. Hyperintense uterine leiomyoma at T2-weighted MR imaging: differentiation with dynamic enhanced MR imaging and clinical implications. Radiology 1993;189:721—5.
[67] Munro MG, Critchley HOD, Broder MS, Fraser IS. FIGO classification system (palm-coein) for causes of abnormal uterine bleeding in nongravid women of reproductive age. Int J Gynaecol Obstet 2011;113:3—13.
[68] D'Angelo E, Espinosa I, Ali R, Gilks CB, Rijn Mvd, Lee CH, et al. Uterine leiomyosarcomas: tumor size, mitotic index, and biomarkers Ki67, and BCL-2 identify two groups with different prognosis. Gynecol Oncol 2011;121:328—33.
[69] Kawakam S, Togashi K, Konishi I, Kimura I, Fukuoka M, Mori T, et al. Red degeneration of uterine leiomyoma: MR appearance. J Comput Assist Tomogr 1994;18:925—8.
[70] Tsushima Y, Kita T, Yamamoto K. Uterine lipoleiomyoma: MRI, CT and ultrasonographic findings. Br J Radiol 1997;70:1068—70.
[71] Barral M, Placé V, Dautry R, Bendavid S, Cornelis F, Foucher R, et al. Magnetic resonance imaging features of uterine sarcoma and mimickers. Abdom Radiol 2017;42:1762—72.
[72] Thoeny HC, De Keyzer F. Extracranial applications of diffusion-weighted magnetic resonance imaging. Eur Radiol 2007;17:1385—93.
[73] Koyama T, Tamai K, Togashi K. Current status of body MR imaging: fast MR imaging and diffusion-weighted imaging. Int J Clin Oncol 2006;11:278—85.
[74] Bakir B, Bakan S, Tunaci M, Bakir VL, Iyibozkurt AC, Berkman S, et al. Diffusion-weighted imaging of solid or predominantly solid gynaecological adnexial masses: is it useful in the differential diagnosis? Br J Radiol 2011;84:600—11.
[75] Parker WH, Fu YS, Berek JS. Uterine sarcoma in patients operated on for presumed leiomyoma and rapidly growing leiomyoma. Obstet Gynecol 1994;83:414—8.
[76] Bell SW, Kempson RL, Hendrickson MR. Problematic uterine smooth muscle neoplasms: a clinicopathologic study of 213 cases. Am J Surg Pathol 1994;18:535—58.
[77] Wang F, Wang Y, Zhou Y. Comparison between types Ii and II epithelial ovarian cancer using histogram analysis of

monoexponential, biexponential, and stretched-exponential diffusion models. J Magn Reson Imaging 2017;46:1797.
[78] Wibmer A, Hricak H, Gondo T. Haralick texture analysis of prostate MRI: utility for differentiating non-cancerous prostate from prostate cancer and differentiating prostate cancers with different gleason scores. Eur Radiol 2015;25:2840.
[79] Kusunoki S, Terao Y, Ujihira T, Fujino K, Kaneda H, Kimura M, et al. Efficacy of PET/CT to exclude leiomyoma in patients with lesions suspicious for uterine sarcoma on MRI. Taiwan J Obstet Gynecol 2017;56:508—13.
[80] Sadeghi R, Zakavi SR, Hasanzadeh M, Treglia G, Giovanella L, Kadkhodayan S. Diagnostic performance of fluorine-18-fluorodeoxyglucose positron emission tomography imaging in uterine sarcomas: systematic review and meta-analysis of the literature. Int J Gynecol Cancer 2013;23:1349—56.
[81] Flier J, Mueckler M, Usher P, Lodish H. Elevated levels of glucose transport and transporter messenger RNA are induced by RAS or SRC oncogenes. Science 1987;235:1492—5.
[82] Oehr P. Metabolism and transport of glucose and fdg. In: Ruhlman JOP, Bieersack H, editors. PET in oncology: basic and clinical applications. Berlin: Springer; 1999. p. 43—57.
[83] Umesaki N, Tanaka T, Miyama M, Kawamura N, Ogita S, Kawabe J, et al. Positron emission tomography with (18)f-fluorodeoxyglucose of uterine sarcoma: a comparison with magnetic resonance imaging and power Doppler imaging. Gynecol Oncol 2001;80:372—7.
[84] Chura JC, Truskinovsky AM, Judson PL, Johnson L, Geller MA, Downs Jr LS. Positron emission tomography and leiomyomas: clinicopathologic analysis of 3 cases of PET scan-positive leiomyomas and literature review. Gynecol Oncol 2007;104:247—52.
[85] Kitajima K, Murakami K, Yamasaki E, Kaji Y, Sugimura K. Standardized uptake values of uterine leiomyoma with 18F-FDG PET/CT: variation with age, size, degeneration, and contrast enhancement on MRI. Ann Nucl Med 2008;22:505—12.
[86] Yamane T, Takaoka A, Kita M, Imai Y, Senda M. 18F-FLT PET performs better than 18f-fdg pet in differentiating malignant uterine corpus tumors from benign leiomyoma. Ann Nucl Med 2012;26:478—84.
[87] Bélissant O, Champion L, Thevenet H, Weinmann P, Alberini J-L. Value of 18F- PET/CT imaging in the staging, restaging, monitoring of response to therapy and surveillance of uterine leiomyosarcomas. Nucl Med Commun 2018;39:652—8.
[88] Macciò A, Kotsonis P, Chiappe G, Melis L, Zamboni F, Madeddu C. Long-term survival in a patient with abdominal sarcomatosis from uterine leiomyosarcoma: role of repeated laparoscopic surgery in treatment and follow-up. J Minim Invasive Gynecol 2016;23:1003—8.
[89] Ho KC, Lai CH, Wu TI, Ng KK, Yen TC, Lin G, et al. 18F-fluorodeoxyglucose positron emission tomography in uterine carcinosarcoma. Eur J Nucl Med Mol Imaging 2008;35:484—92.
[90] Park JY, Kim EN, Kim DY, Suh DS, Kim MY, Kim HJ, et al. Role of PET or PET/CT in the post-therapy surveillance of uterine sarcoma. Gynecol Oncol 2008;109:255—62.
[91] Park JY, Lee JW, Lee HJ, Lee JJ, Moon SH, Kang SY, et al. Prognostic significance of preoperative 18F-FDG PET/CT in uterine leiomyosarcoma. J Gynecol Oncol 2017;28:e28.
[92] Prat J. Figo staging for uterine sarcomas. Int J Gynaecol Obstet 2009;104:177—8.
[93] Amant F, Coosemans A, Debiec-Rychter M, Timmerman D, Vergote I. Clinical management of uterine sarcomas. Lancet Oncol 2009;10:1188—98.